Analysis of Mesocyclone Detection Algorithm Attributes to Increase Tornado Detection

Christina M. Nestlerode[1,2,3]

and

Michael B. Richman[4]

Research Experience for Undergraduates Final Project

Last Revised: July 31, 2003

[1]OWC REU Program
Norman, Oklahoma

[2]OU School of Meteorology
Norman, Oklahoma

[3]Lycoming College
Department of Physics and Astronomy
700 College Place
Box #1014
Williamsport, PA 17701
neschri@lycoming.edu

[4]The University of Oklahoma
School of Meteorology
100 East Boyd Street
Norman, OK 73019
mrichman@ou.edu

Abstract

The Mesocyclone Detection Algorithm (MDA) is used in the Weather Surveillance Radar –1988 Doppler (WSR-88D) to detect rotation associated with tornadoes and other severe weather. The MDA analyzes Doppler radar radial velocity volume scans to compose a number of attributes thought to be related to mesocyclone formation. The 23 attributes of the MDA are compared to truthed tornado data in exploratory and diagnostic analyses to examine the underlying structure of the MDA.

Results of these analyses indicate that the MDA is a highly correlated system with a wide variety of complexity in those correlations. This multicollinearity can hinder statistical prediction. Measured associations between the attributes vary from near zero correlation to complex correlations with values greater than 0.8, binding up to nine MDA attributes. In diagnostic analyses, linear and logistic regressions are performed on various sets of MDA attributes in an attempt to distinguish tornado events from non-tornado events. Logistic regression is found to be the most successful model due to its parsimony and ability to classify correctly tornado versus non-tornado cases.

This research has shown that the number of attributes in the MDA can be decreased by projecting the 23 correlated attributes on a number of uncorrelated dimensions. Using principal component analysis (PCA), multivariate exploration of the data determines that 9 dimensions are needed to describe 85% of the variability of the MDA attributes. While the MDA is currently an improvement over older algorithms, this research shows that it is advantageous to reduce the redundancy of the MDA to make it a more useful tool.

1. Introduction

With the advent of a national network of Doppler radar capable of sensing small circulation scales undiscovered until the last decade, the detection of mesocyclones has received considerable attention in recent years. A mesocyclone can take on various definitions, one of which is a storm-scale region of rotation, typically around 2-6 miles in diameter and often found in the right rear flank of a supercell (Branick 2003). Alternatively, the term mesocyclone, as used in Doppler radar studies, is defined as a rotation signature with measurable magnitude, vertical depth, and duration (Branick 2003). Mesocyclones are of particular interest since tornadoes, large hail, and damaging winds are collocated with the rotation area. These hazards lead to unnecessary loss of life and destruction of property if people are not adequately warned of the threat. Therefore, a significant proportion of mesocyclone studies (e.g. Desrochers and Donaldson 1992, Lee and White 1998, Tipton et al. 1998, and Jones 2002) have addressed the development of radar algorithms that can assist forecasters in predicting tornadoes and warning people of imminent danger. Improvements in radar and algorithm technology have increased lead time (time between the forecast of a tornado and its appearance) from a few minutes a decade ago to eleven minutes in the past few years (Trafalis et al. 2003). Despite this, tornados still kill and injure people due to insufficient warning time, misdetection, and complacency of the public ignoring repeated false alarms (the number of tornadoes that an algorithm predicts that fail to materialize). Additional lives will be saved if computer algorithms that identify mesocyclones are improved; the goal of our project is to investigate the efficiency of the current radar Mesocyclone Detection Algorithm. If the algorithm can be improved or simplified, that should result in increased lead times and lower false alarm rates.

Detection algorithms exist within the Weather Surveillance Radar-1988 Doppler (WSR-88D) system to find areas of rotation in severe thunderstorms. One of the algorithms, the

Mesocyclone Detection Algorithm (MDA), described by Stumpf et al. (1998), is in use to replace the WSR-88D Build 9.0 Mesocyclone Algorithm (Zrnić et al. 1985). The older algorithm, WSR-88D Build 9.0 Mesocyclone Algorithm (WSR-88D B9MA), has been found to be incapable of detecting a number of mesocyclones because they are weaker than the threshold strength of the algorithm, even though such rotations can produce tornadoes. Also, the WSR-88D B9MA misclassifies many strong non-tornadic rotations by deducing tornado existence within the rotation and hence, producing high false alarm rates in the range of 73.9 to 96.6 percent (Stumpf et al. 1998). The older algorithm looks for specific rotations as potentially tornadic, whereas the MDA offers a new approach.

Stumpf et al. (1998) recognized that a new algorithm should detect storm rotations from 1-10 km in diameter to catch even seemingly insignificant rotation. Moreover, instead of instant analysis of rotation, the MDA output scrutinizes each case for tornado development potential. Other enhancements include new threshold definitions, improved vertical association, and the introduction of association to features detected on radar volume scans.

Despite numerous improvements to the old algorithm, the MDA is not perfect. Trafalis et al. (2003) state that the MDA has problems with the underdetection of tornadoes as well as the high false alarm rate. Stumpf et al. (1998) calculate a false alarm rate for the MDA ranging from 67.7 to 75.7 percent. Furthermore, the MDA attributes have an unknown degree of redundancy, since there are a large number of variables that comprise the MDA and many of them are connected through Doppler velocity. It may be possible to reduce the number of attributes while maintaining the accuracy of the MDA. By accomplishing such a goal, it will be easier for a forecaster, who is under critical time constraint, to use the MDA more effectively in predicting tornado formation.

Section 2 of this paper describes the data sets used. Section 3 discusses the variety of methodologies that were applied in the research, Section 4 illustrates the results of the research, and Section 5 presents the discussion of the results. The paper ends with Section 6, which is conclusions from the research and suggestions for future lines of investigation.

2. Data

Two primary data sets are used in this research. The first is truthed tornado data collected and verified by the National Severe Storms Laboratory (NSSL) through ground damage reports (Stumpf et al. 1998). Twenty-three out of 24 MDA attributes measured for 2259 truthed tornado cases are selected for the study. A second data set contains non-tornado data of the same 23 MDA attributes for 63,116 cases. The MDA attributes, defined by Stumpf et al. (1998), are derived from Doppler radar radial velocity volume scans. Before the data are processed, artifacts such as noise or incorrectly dealiased velocities in the volume scans are removed. All velocities with reflectivity values below 20 dBZ are deleted and then an existing scheme within the WSR-88D removes improperly dealiased velocities according to the threshold of the program (Eilts and Smith 1990). The first step of the MDA creates shear segments by looking at cyclonic shear patterns in the Doppler volume scans. Then, velocity difference and maximum gate-to-gate velocity difference are calculated from the shear segments. The next step moves into 2-dimensional (2D) analyses, and feature core extraction (Stumpf et al. 1998) is used to define shear features horizontally. From these data, the rotational velocity of the detected vorticity (rotation about a vertical axis) is computed. Then, a new vertical association technique is applied to the 2D features to view the vortex in a 3-dimensional (3D) form. In the last step, a time dimension is added to the 3D components if a feature appears on more than one consecutive

volume scan. From the MDA analyses, data used in this study contain 23 attributes, listed in Table 1 (adapted from Trafalis et al. 2003) and described in Appendix A.

3. Methodology

The primary goals of the project are exploratory data analysis of the MDA as well as diagnosis of tornado versus non-tornado events. Accordingly, it is important to compare directly tornado cases and non-tornado cases. From the non-tornado data, 2259 cases are randomly selected to have the same number of observations as the tornado data set. By creating a data set with as many tornadoes as non-tornadoes, the techniques applied to these data have the opportunity to be unbiased.

Exploratory data analysis is carried out at the univariate, bivariate, and multivariate levels. All analyses are performed using S-Plus 2000. For univariate analyses, histograms of the tornado and non-tornado cases are created. For comparison purposes, each attribute is plotted on the same scale for both data sets, making it possible to overlay and compare the histograms for tornado and non-tornado cases. Bivariate data analysis of the MDA attributes is carried out by visual inspection of scatterplots and through calculation of Pearson correlations. Multivariate analysis makes use of principal components (PC) to discover the underlying number of dimensions of the MDA and the correlation structure of these dimensions. The fundamental equation of principal component analysis (PCA) is $\mathbf{Z} = \mathbf{F}\mathbf{A}^{T}$ where $\mathbf{Z}$ is a matrix of the standardized MDA data of order n x m where n is the number of cases and m is the number of attributes, $\mathbf{F}$ is the matrix of the PC score time series of order n x p where p is the number of PCs retained, and $\mathbf{A}$ is the matrix of the PC loadings that portray which attributes cluster together on each dimension. The matrix $\mathbf{A}$ is of order m x p (Richman 1986). PCA is performed in multiple steps. The first step involves relating the data. Since the MDA data are measured on different

metrics, they are standardized implicitly by forming a 23 x 23 correlation matrix, **R**. The correlation matrix is decomposed into eigenvectors, **V**, and eigenvalues, **D,** according to the following equation $\mathbf{R} = \mathbf{A}\mathbf{A}^T$ where $\mathbf{A} = \mathbf{V}\mathbf{D}^{1/2}$. Since the goal is the compact description of the MDA's correlation structure, a Varimax orthogonal rotation is applied to determine which attributes cluster on specific dimensions. The second step involves determining the optimal number of PC dimensions (p) to rotate based on minimizing the number of misclassifications of the clustering of attributes as depicted in **R**. A plausible range of solutions is identified for p = 4,5,…,10 and each solution is tested for the number of misclassified attributes. The classification process is defined by binarizing the rotated PC loadings where a loading with an absolute value ≥ 0.5 is considered "in the cluster" and coded as 1. Those loadings with an absolute value < 0.5 are considered "out of the cluster" and coded as 0. The philosophy behind this approach is given in Richman and Gong (1999). Similarly, those values in **R** with an absolute value ≥ 0.5 are considered in the cluster and those correlations with an absolute value < 0.5 are considered out of the cluster and coded as 1 and 0, respectively. In cases where a 0 in the loadings are matched to a 1 in the correlations or vice versa, these are coded as misclassifications. The dimension number associated with the lowest number of misclassifications is selected as the optimal p.

Another way of assessing misclassification is through the use of regression. Linear and logistic regressions are applied to the 23 MDA attributes. Linear regression is used as a baseline to determine the amount of linear relation between the attributes in discriminating tornadoes from non-tornadoes, whereas, logistic regression is a non-linear type of regression where the dependant variable is a dummy variable labeled 0 or 1. If the event occurs, the variable is one number, if it does not, the variable is the other number. In this way, data with only two outcomes

can be analyzed easily (Wilks 1995). A stepwise process is used to preprocess the linear regression by eliminating those attributes that do not provide significant residual sum of squares (RSS) to the variance explained. Those attributes with significant RSS, as tested by an t-statistic, are retained and inserted into the linear regression model. A similar process is used to reduce the number of MDA attributes in the logistic regression based on the amount of deviance explained. Those attributes with significant deviance are retained and inserted into the logistic regression model that is analyzed physically. Another measure of regression model performance is R^2 (Wilks 1995). The counterpart to R^2 for logistic regression is called the pseudo R^2, defined as 1-(Residual Deviance/Null Deviance). A standardization preprocessing is performed on the data before the logistic regression. The data are scaled by shifting each attributes mean to zero, the variance to be one, and the skew to be close to zero. After the standardization procedure, Box-Cox transformations are performed on the data to remove skewness and help meet the distributional assumptions of the regression. For testing purposes, the tornado data was split into two parts. The first half is used as training data to select a model to predict the second half using both linear and logistic regressions. Likewise, the second half is used as training data to predict the first half. By doing so, the stability of the model coefficients can be examined.

Misclassification analysis is applied to the regressions in the following process. The predictions of the regressions are binarized (1,0) where a 1 represents a tornado prediction and a 0 represents a non-tornado prediction. These are compared directly to the truthed data and tallied.

4. Results

Histograms provide basic information on the shape of the distributions for the tornado and non-tornado data sets (Figure 1). When visually assessing histograms showing the radar detected mesocyclone base, there is a striking difference between the two data sets (Figure 1a). The non-tornado cases (left column) are dominated by bases at 400 m or less whereas tornado cases have a more even distribution of base heights, with a maximum around 1000 m. There is a considerable amount of overlap between the distributions for the two sets. Comparison of the depth (Figure 1b) show most of the non-tornado cases at depths less than 2000 m, as opposed to the tornado cases that exist in the range of approximately 2000 to 12000 m. When looking at strength rank (Figure 1c), there is considerable overlap between the two sets from ranks 1 to 6. The zero rank is mainly comprised of non-tornadoes while ranks above 5 are generally tornado cases. In low-level diameter (Figure 1d), there is a large amount of overlap between the two sets. There is a greater number of non-tornadoes at small low-level diameters than tornadoes. At least half of the distribution overlaps in maximum diameter (Figure 1e). Despite the overlap in the right tails of the two sets, many of the non-tornado cases heights of maximum diameter (Figure 1f) occur at below 2000 m. There is less low-level rotational velocity in the non-tornado cases, but there is a large overlap between the distributions of the two sets (Figure 1g). Similar results can be seen for maximum rotational velocity (Figure 1h). Histograms of the height of maximum rotational velocity (Figure 1i), show a broad maximum in the tornado cases between 1000 and 4000 m. In low-level shear and maximum shear, the two distributions are almost identical (Figures 1j and 1k). Similar to Figure 1i, height of maximum shear (Figure 1l) shows a spike in the non-tornado cases at values lower than 2000 m, and a broad maximum for tornado cases from 500 to 4000 m. Low-level gate-to-gate velocity difference (Figure 1m) indicates less

overlap than shear, and the non-tornado cases seem to decrease after 30 ms^{-1}, while the tornado cases are evident until 55 ms^{-1}. Maximum gate-to-gate velocity difference (Figure 1n) shows that the two distributions are offset more than in the low-level gate-to-gate velocity difference distributions. Non-tornado cases are scarce after 40 ms^{-1} whereas tornado cases appear until 65 ms^{-1}. Height of maximum gate-to-gate velocity difference (Figure 1o) shows a peak in non-tornado cases below 2000 m. Core base histograms (Figure 1p) illustrate similarities to previous height parameters, but there are fewer non-tornado cases in the mid levels. Core depth (Figure 1q) is striking as no tornado cases occur below 3000 m, while a majority of the non-tornado cases are at less than 2000 m. The shape of the distribution of tornado cases and non-tornado cases is similar when looking at age (Figure 1r), but non-tornadoes decrease rapidly in number after 30 min while some tornado cases exist up to 100 min. Strength index is an attribute that shows overlap between the two data sets with some separation below 2000 m and above 4000 m (Figure 1s). Strength index "rank" has considerable overlap in ranks from 0 to 3, however, there are many more tornado cases with ranks greater than 4 (Figure 1t). Figure 1u depicts that tornado cases have significant relative depth when compared with non-tornado cases. There is some overlap in the middle of the distributions, but the left part of the distribution illustrates a striking peak in non-tornado cases. Low-level and mid-level convergence are unique attributes because they are both bimodal. However, low-level convergence (Figure 1v) shows a peak in non-tornadoes at lower values if the zeros are ignored, whereas mid-level convergence shows an overlap between the two sets (Figure 1w).

Bivariate analysis though scatterplots indicated a large range of associations between the pairs of MDA variables (not shown). Many of the 23 MDA attributes are highly correlated within the tornado and non-tornado data sets. In the tornado data set (Table 2), Pearson

correlation calculations establish strong relationships (defined as absolute correlations exceeding 0.75), especially between the three strength parameters (attributes 3, 19, 20), rotational velocities (attributes 7 and 8), and gate-to-gate velocity differences (attributes 13 and 14). In the non-tornado cases (Table 3), a greater number of high correlations occur with emphasis on height parameters (attributes 6, 9, 12, 15, and 16). There are inherent differences in the correlation structures of the tornado and non-tornado data. For example, the tornado data shows correlations between base, core base, and a negative relationship with low-level convergence, while in the non-tornado cases, base is related to depth, strength rank, height of maximum diameter, height of maximum rotational velocity, height of maximum shear, height of maximum gate-to-gate velocity difference, core depth, relative depth and low-level divergence.

There is a range in complexity of the underlying correlation structure of the data. As seen in Figure 2a, some attributes are not correlated with any others. The complexity then increases, as some attributes are correlated with one other, some are associated with two others, and some are related to four other attributes (Figure 2b). The most complex case involves more than eight variables where most are associated with all other attributes (Figure 2c).

Multivariate analysis using PCA determines how many underlying attributes are needed to account for a substantial proportion of the variability of the MDA attributes and to summarize the correlation structure of the attributes. For the tornado cases, the optimal p is found to be 9 with one misclassification (Table 4). With 9 dimensions, 85 percent of the total MDA variance is represented using only 39 percent of the data. The variables that cluster together for PC 1 through 9 are shown (Table 6). On the first PC are strength rank, low-level rotational velocity, maximum rotational velocity, low-level shear, maximum shear, low-level gate-to-gate velocity difference, maximum gate-to-gate velocity difference, strength index and strength index “rank”.

Since some of the velocity parameters are used to define the strength indices and ranks (see Appendix A), this PC is loading the attributes related to "circulation strength". The second PC accounts for "circulation base characteristics" as it contains base, core base, and negative low-level convergence. The third PC is depth, height of maximum diameter, and relative depth, so it is a measure of "circulation volume". Low-level shear and negative low-level diameter comprise the fourth PC and represent the "low-level circulation" characteristics of the storm. The fifth PC is a "circulation height" measure as it contains height of maximum rotational velocity, height of maximum shear, height of maximum gate-to-gate velocity difference, and core base. PCs 6 through 9 are associated with single attributes and can be named accordingly. The sixth PC loads only age. Core depth comprises the seventh PC, mid-level convergence is on the eighth PC, and maximum diameter loads on the ninth PC. Each of the nine PCs have an associated PC score that described the time behavior of each cluster of attributes (PCs 1 – 5) or single attributes (PCs 6 -9). Any individual tornado can therefore be profiled by examining the PC scores for that case. By doing so, it is possible to distinguish tornadoes with greater than average low level circulation from those with large circulation volume (Figure 3).

The optimal p for the non-tornado cases is 5 and that is associated with 6 misclassifications. Five dimensions account for 78.5 percent of the variance of the MDA attributes and only 21.7 percent of the data. Other dimensions are analyzed, but they have more misclassification as seen in Table 5. The first PC is a representation of "depth and height" of the non-tornado cases since it contains base, depth, strength rank, height of maximum diameter, height of maximum rotational velocity, height of maximum shear, height of maximum gate-to-gate velocity difference, core base, core depth, relative depth, and low-level convergence (Table 7). The second PC is composed of low-level rotational velocity, maximum rotational velocity,

maximum gate-to-gate velocity difference, strength index, and strength index "rank", so it represents strength. Negative low-level diameter and maximum diameter load with low-level shear and maximum shear on the third PC, making it a glimpse of low-level characteristics of the storm. The fourth PC has strength rank, age, relative depth, and mid-level convergence, so it shows the weakness of the mesocyclone. The fifth PC is a velocity parameter, since it loads low-level rotational velocity and low-level gate-to-gate velocity difference.

The regression analyses combine the tornado and non-tornado data to diagnose which attributes (known as predictors) are best suited to distinguishing between the two. Twelve significant linear regression attributes are determined using the t-test (Table 8). The most significant attribute according the t-statistic is strength rank. Age, core depth, and relative depth also predict the variance well, with high t-values. In linear regression, the R^2 of the first half of the data predicting the second half is 0.5666. Using the second half to predict the first half, the R^2 value is 0.5456. In logistic regression, the nine most important attributes are determined through explained deviance. Table 9 shows that the most significant attributes are strength rank, age and base, all with t-values above 5 (highly significant). The pseudo R^2 for the first half of the data predicting the second half is 0.5306 and 0.5105 for the second half of the data predicting the first. All of the attributes in logistic regression also appear in linear regression, but linear includes maximum rotational velocity, height of maximum rotational velocity, and height of maximum gate-to-gate velocity difference. In the ability to distinguish correctly tornadoes from non-tornadoes, logistic regression has better results than linear regression by .6 percent (Table 10). Logistic regression is considered the superior technique because it is a more accurate classifier and uses fewer predictors to achieve that level of classification.

5. Discussion

The histogram results show a number of important features of the MDA, especially concerning attributes whose distributions between tornado and non-tornado cases do not separate well. Low-level diameter is not a good discriminator because there is a extensive overlap between the two data sets. Similarly, low-level rotational velocity, maximum rotational velocity, low-level shear, maximum shear, low-level gate-to-gate velocity difference, maximum gate-to-gate velocity difference, and strength index have significant overlap in the distributions of the two cases. Interestingly, low-level shear and maximum shear histograms are almost identical, meaning that there is no need for two separate discriminators of shear. Another intriguing feature of the MDA attributes are the height parameters. There are prominent peaks in the non-tornado cases of base, height of maximum diameter, height of maximum rotational velocity, height of maximum shear, height of maximum gate-to-gate velocity difference, core base, and relative depth. Tornadoes tend to occur with higher bases, maximum diameters, and core bases; they also tend to have velocity components higher in the storm. There is also a broader range of heights in tornado cases. Another promising discriminator is core depth because there is a striking lack of overlap in the histograms of the two data sets. In tornado cases, core depth is almost always above 3000 m while non-tornado storms have core depths below 2000 m. Age has almost a complete overlap between the two sets, but tornado cases to tend to last longer because they may survive for up to 100 minutes while non-tornado features last no longer than 30 minutes. Strength rank and strength index "rank" histograms are similar because tornadoes have strengths much higher than non-tornadoes do.

The PCA results are consistent with the correlation matrix since the same variables are correlated as those that are grouped on a PC. For example, the correlation matrix shows that

height of maximum rotational velocity, height of maximum shear, height of maximum GTGVD, and core base are all highly positively associated and the same group of attributes represents the second PC. Also, the regression results pull out the same significant variables as the correlation matrix and the PCA. The two sets of regression results are stable; therefore, this leads credence to the models being stable.

6. Conclusions

The correlation results suggest that the MDA is overdetermined and complex in that most of the attributes are associated strongly with each other. The PCA has the ability to draw the meaningful structures out of the complicated correlation matrix. Twenty three attributes are replaced by 9 orthogonal dimensions resulting in a more compact conceptual model of the MDA. Interestingly, the number of dimensions given by the PCA is same as the number of predictors given by the logistic regression. Each rotated PC is interpreted as a physically meaningful structure that relates well to the clusters of variables in the parent correlation matrix. These, in turn, relate to rotation of the atmosphere. Furthermore, the PC model provides a time series of each of these new dimensions. Individual tornado profiles are a unique classification tool, showing the tornado's strengths and weaknesses in the range of each PC. The combination of PC loadings, identifying clusters of highly correlated MDA attributes for physical interpretation and PC scores that express the time behavior of the new uncorrelated variables, offers an exciting line of investigation in profiling tornadic events based on which types of atmospheric behavior are associated with different types of storms. Based on the consistency among several types of statistical investigations, the results suggest that the MDA can be simplified without loss of accuracy.

Acknowledgements: This work was funded by National Science Foundation grant NSF 0097651. A portion of Dr. Richman's time was supported by NSF Grant EIA-0205628. The lead author would like to thank Daphne Zaras and the REU selection committee, Greg Stumpf at NSSL for his support and patience, Philip Bothwell and Kim Elmore for help with S-Plus, Becca Mazur for her support with Quality Control, Mark Laufersweiler for help and advice, and all of the REU/ORISE/SCEP students who made the summer as extreme as possible.

Appendix A

The 23 MDA attributes are measurements gleaned from Doppler radial velocity data. Base is the height above radar level (ARL) of the lowest 2D elevation scan. By adding half-power beamwitdth to the top and bottom of the final 3D feature, depth is calculated. Strength rank is a dimensionless number ranging from 1 to 25 that is first applied to the 1D shear segments, and later adjusted after the 2D elevation scans are analyzed. The strength of the vortex is determined by preset thresholds in velocity difference and shear, or gate-to-gate velocity difference based on Philips Laboratory and early MDA criteria. Low-level diameter (D) is the distance between the maximum outbound velocity (V_{max}) and maximum inbound velocity (V_{min}) at the lowest 2D elevation scan. Maximum diameter is the distance between V_{max} and V_{min} at the greatest diameter from all features below 12 km. Height of maximum diameter is the altitude at which the maximum diameter is measured. Low-level rotational velocity (V_r) is (V_{max}- V_{min})/2 at the lowest altitude 2D elevation scan. Maximum rotational velocity is the highest value of (V_{max}- V_{min})/2 through all volume scans. Height of maximum rotational velocity is the altitude at which the maximum rotational is found. Low-level shear is V_r /D at the lowest 2D feature. Maximum shear is the highest value of V_r /D. Height of maximum shear is the altitude at which maximum shear is measured. Low-level gate-to-gate velocity difference (GTGVD) is the

lowest elevation scan measure of greatest velocity difference between adjacent velocity values in the original shear segment. The greatest GTGVD in the whole storm is the maximum GTGVD. Where maximum GTGVD is measured is the height of maximum GTGVD. Core base and core depth are the measures of the lowest elevation scan ARL and the depth at the determined vertical core, which is defined by its strength rank. Age is the fourth dimension of the MDA output; it is a measure of the amount of time that the rotation exists. Mesocyclone Strength Index (MSI) is a strength index that is measured by integrating the previously determined strength ranks and multiplying by 1000. Each strength rank is weighted based on air density so that more emphasis is given to 2D features at lower heights. The MSI is normalized by dividing it by the total depth of the 3D feature. Strength index (MSIr) "rank" is a non-dimensional number ranging from 1 to 25 to correct to the strength index for range sampling limitations. Relative depth is an attribute taken from the NSSL SCIT algorithm (Johnson et al. 1998) or sounding data and it is the percentage of the depth of the storm cell. Low-level and mid-level convergence are measured from the average of the radial convergence shear segment velocity differences in the 2D features (adapted from Stumpf et al. 1998).

References

Branick, M., cited 2003: A Comprehensive Glossary of Weather Terms for Storm Spotters. [Available online at http://www.srh.noaa.gov/oun/severewx/glossary.php.]

Desrochers, P. R. and R. J. Donaldson, 1992: Automatic Tornado Prediction with an Improved Mesocyclone-Detection Algorithm. *Weather and Forecasting,* **7,** 373–388.

Eilts, M. D., and S. D. Smith, 1990: Efficient Dealiasing of Doppler Velocities Using Local Environment Constraints. *Journal of Atmospheric and Oceanic Technology,* **7,** 118-128.

Johnson, J. T., P. L. MacKeen, A. Witt, E. D. Mitchell, G. J. Stumpf, M. D. Eilts, K. W. Thomas, 1998: The Storm Cell Identification and Tracking Algorithm: An Enhanced WSR-88D Algorithm. *Weather and Forecasting,* **13,** 263–276.

Jones, T. A., 2002: Verification of the NSSL Mesocyclone Detection Algorithm: A Climatological Perspective. Unpublished MS Thesis, University of Oklahoma, Norman, OK, 235pp.

Lee, R. R., and A. White, 1998: Improvement of the WSR-88D Mesocyclone Algorithm. *Weather and Forecasting,* **2,** 341–351.

Richman, M. B., 1986: Rotation of Principal Components. *Journal of Climatology,* **6,** 293-335.

Richman, M.B, and X. Gong, 1999: Relationships between the Definition of the Hyperplane Width to the Fidelity of Principal Component Loading Patterns. *Journal of Climate,* **12,** 1557-1576.

Stumpf, G. J., A. Witt, E. D. Mitchell, P. L. Spencer, J. T. Johnson, M. D. Eilts, K. W. Thomas, and D. W. Burgess, 1998: The National Severe Storms Laboratory Mesocyclone Detection Algorithm for the WSR-88D. *Weather and Forecasting,* **13,** 304-326.

Tipton, G. A., E. D. Howieson, J. A. Margraf, and R. R. Lee, 1998: Optimizing the WSR-88D Mesocyclone/Tornadic Vortex Signature Algorithm using WATADS—A case study*. *Weather and Forecasting,* **3,** 367–376.

Trafalis, T.B., B. Santosa and M.B. Richman, 2003: Tornado detection with kernel-based methods**.** *Intelligent Engineering Systems Through Artificial Neural Networks*, ASME Press, **13**, in press.

Wilks, D. S., 1995: *Statistical Methods in the Atmospheric Sciences.* R. Dmowska and J. R. Holton, Academic Press, 160-181.

Zrnić, D. S., D. W. Burgess, and L. D. Hennington, 1985: Automatic detection of mesocyclonic shear with Doppler radar. *Journal of Atmospheric and Oceanic Technology,* **2,** 425-438.
Table 1. List of 23 Mesocyclone Detection Algorithm attributes.

1. base (m) [0-12000]	13. low-level gate-to-gate velocity difference (m/s) [0-130]
2. depth (m) [0-13000]	14. maximum gate-to-gate velocity difference (m/s) [0-130]
3. strength rank [0-25]	15. height of maximum gate-to-gate velocity difference (m) [0-12000]
4. low-level diameter (m) [0-15000]	16. core base (m) [0-12000]
5. maximum diameter (m) [0-15000]	17. core depth (m) [0-9000]
6. height of maximum diameter (m) [0-12000]	18. age (min) [0-200]
7. low-level rotational velocity (m/s) [0-65]	19. strength index (MSI) weighted by average density of integrated layer [0-13000]
8. maximum rotational velocity (m/s) [0-65]	20. strength index (MSIr) “rank” [0-25]
9. height of maximum rotational velocity (m) [0-12000]	21. relative depth (%) [0-100]
10. low-level shear (m/s/km) [0-175]	22. low-level convergence (m/s) [0-70]
11. maximum shear (m/s/km) [0-175]	23. mid-level convergence (m/s) [0-70]
12. height of maximum shear (m) [0-12000]	

Table 2. Correlation matrix for tornado cases. The absolute value of darker shaded coefficients exceeds 0.75, while the absolute value of the lighter shaded coefficients is between 0.50 and 0.74.

	1	2	3	4	5	6	7	8	9	10	11	12	13	14	15	16	17	18	19	20	21	22	23
1	1.00	0.20	0.05	0.35	0.19	0.32	-0.14	-0.29	0.39	-0.27	-0.41	0.42	0.04	-0.12	0.45	0.80	0.08	-0.13	-0.26	-0.20	0.01	-0.69	-0.29
2	0.20	1.00	0.29	0.01	0.35	0.60	0.11	0.24	0.42	0.04	0.04	0.36	0.18	0.27	0.36	0.33	0.39	0.08	0.17	0.34	0.53	-0.05	0.20
3	0.05	0.29	1.00	-0.11	0.06	0.27	0.67	0.70	0.02	0.37	0.41	-0.01	0.62	0.69	0.02	0.16	-0.19	0.11	0.84	0.80	0.43	0.18	0.32
4	0.35	0.01	-0.11	1.00	0.42	-0.19	-0.12	-0.17	0.13	-0.64	-0.44	0.43	-0.27	-0.26	0.25	0.29	0.05	-0.10	-0.20	-0.29	-0.04	-0.31	-0.18
5	0.19	0.35	0.06	0.42	1.00	0.26	-0.02	0.08	0.25	-0.23	-0.22	0.21	-0.08	-0.05	0.21	0.22	0.16	-0.02	-0.01	-0.02	0.23	-0.14	-0.01
6	0.32	0.60	0.27	-0.19	0.26	1.00	0.09	0.15	0.35	0.10	0.01	0.13	0.21	0.23	0.25	0.36	0.22	0.05	0.14	0.27	0.36	-0.15	0.10
7	-0.14	0.11	0.67	-0.12	-0.02	0.09	1.00	0.72	-0.31	0.55	0.49	-0.24	0.85	0.72	-0.29	-0.25	-0.08	0.12	0.77	0.70	0.28	0.35	0.37
8	-0.29	0.24	0.70	-0.17	0.08	0.15	0.72	1.00	-0.01	0.43	0.55	-0.10	0.58	0.83	-0.04	-0.16	0.00	0.12	0.86	0.83	0.35	0.40	0.45
9	0.39	0.42	0.02	0.13	0.25	0.35	-0.31	-0.01	1.00	-0.23	-0.19	0.47	-0.20	-0.06	0.62	0.53	0.31	-0.07	-0.10	0.02	0.15	-0.33	-0.09
10	-0.27	0.04	0.37	-0.64	-0.23	0.10	0.55	0.43	-0.23	1.00	0.72	-0.38	0.61	0.51	-0.29	-0.30	-0.08	0.10	0.49	0.48	0.15	0.36	0.23
11	-0.41	0.04	0.41	-0.44	-0.22	0.01	0.49	0.55	-0.19	0.72	1.00	-0.24	0.44	0.61	-0.20	-0.34	-0.07	0.11	0.60	0.60	0.16	0.44	0.30
12	0.42	0.36	-0.01	0.43	0.21	0.13	-0.24	-0.10	0.47	-0.38	-0.24	1.00	-0.22	-0.10	0.60	0.50	0.20	-0.07	-0.15	-0.09	0.09	-0.32	-0.11
13	0.04	0.18	0.62	-0.27	-0.08	0.21	0.85	0.58	-0.20	0.61	0.44	-0.22	1.00	0.76	-0.25	-0.09	-0.04	0.12	0.65	0.62	0.28	0.22	0.33
14	-0.12	0.27	0.69	-0.26	-0.05	0.23	0.72	0.83	-0.06	0.51	0.61	-0.10	0.76	1.00	-0.03	-0.06	0.00	0.12	0.79	0.80	0.35	0.31	0.44
15	0.45	0.36	0.02	0.25	0.21	0.25	-0.29	-0.04	0.62	-0.29	-0.20	0.60	-0.25	-0.03	1.00	0.58	0.24	-0.07	-0.11	-0.03	0.10	-0.35	-0.10
16	0.80	0.33	0.16	0.29	0.22	0.36	-0.25	-0.16	0.53	-0.30	-0.34	0.50	-0.09	-0.06	0.58	1.00	0.00	-0.09	-0.17	-0.08	0.12	-0.58	-0.19
17	0.08	0.39	-0.19	0.05	0.16	0.22	-0.08	0.00	0.31	-0.08	-0.07	0.20	-0.04	0.00	0.24	0.00	1.00	0.00	-0.07	0.04	0.19	-0.16	0.11
18	-0.13	0.08	0.11	-0.10	-0.02	0.05	0.12	0.12	-0.07	0.10	0.11	-0.07	0.12	0.12	-0.07	-0.09	0.00	1.00	0.12	0.15	0.15	0.12	0.09
19	-0.26	0.17	0.84	-0.20	-0.01	0.14	0.77	0.86	-0.10	0.49	0.60	-0.15	0.65	0.79	-0.11	-0.17	-0.07	0.12	1.00	0.92	0.37	0.38	0.43
20	-0.20	0.34	0.80	-0.29	-0.02	0.27	0.70	0.83	0.02	0.48	0.60	-0.09	0.62	0.80	-0.03	-0.08	0.04	0.15	0.92	1.00	0.43	0.33	0.44
21	0.01	0.53	0.43	-0.04	0.23	0.36	0.28	0.35	0.15	0.15	0.16	0.09	0.28	0.35	0.10	0.12	0.19	0.15	0.37	0.43	1.00	0.11	0.27
22	-0.69	-0.05	0.18	-0.31	-0.14	-0.15	0.35	0.40	-0.33	0.36	0.44	-0.32	0.22	0.31	-0.35	-0.58	-0.16	0.12	0.38	0.33	0.11	1.00	0.21
23	-0.29	0.20	0.32	-0.18	-0.01	0.10	0.37	0.45	-0.09	0.23	0.30	-0.11	0.33	0.44	-0.10	-0.19	0.11	0.09	0.43	0.44	0.27	0.21	1.00

Table 3. Correlation matrix for non-tornado cases. The absolute value of darker shaded coefficients exceeds 0.75, while the absolute value of the lighter shaded coefficients is between 0.50 and 0.74.

	1	2	3	4	5	6	7	8	9	10	11	12	13	14	15	16	17	18	19	20	21	22	23
1	1.00	0.78	0.50	0.38	0.38	0.81	-0.19	-0.22	0.81	-0.33	-0.39	0.81	0.10	0.08	0.83	0.97	0.73	0.25	-0.24	-0.07	0.63	-0.51	0.23
2	0.78	1.00	0.66	0.34	0.46	0.86	-0.19	-0.13	0.84	-0.34	-0.37	0.82	0.10	0.13	0.82	0.82	0.90	0.43	-0.21	0.03	0.76	-0.37	0.44
3	0.50	0.66	1.00	0.24	0.30	0.56	0.15	0.13	0.48	-0.15	-0.19	0.48	0.39	0.37	0.48	0.55	0.60	0.40	0.15	0.32	0.76	-0.10	0.54
4	0.38	0.34	0.24	1.00	0.66	0.20	0.11	0.00	0.28	-0.59	-0.46	0.43	-0.06	-0.09	0.33	0.37	0.33	0.16	-0.03	-0.14	0.32	-0.15	0.16
5	0.38	0.46	0.30	0.66	1.00	0.40	0.02	0.08	0.40	-0.44	-0.43	0.38	-0.05	-0.04	0.38	0.39	0.42	0.19	-0.01	-0.06	0.36	-0.14	0.21
6	0.81	0.86	0.56	0.20	0.40	1.00	-0.20	-0.13	0.83	-0.28	-0.33	0.70	0.10	0.14	0.78	0.84	0.78	0.32	-0.19	0.02	0.65	-0.40	0.31
7	-0.19	-0.19	0.15	0.11	0.02	-0.20	1.00	0.70	-0.29	0.39	0.31	-0.25	0.66	0.49	-0.27	-0.22	-0.21	-0.03	0.64	0.55	0.01	0.34	0.08
8	-0.22	-0.13	0.13	0.00	0.08	-0.13	0.70	1.00	-0.14	0.33	0.43	-0.18	0.43	0.63	-0.15	-0.20	-0.17	-0.03	0.76	0.70	-0.01	0.34	0.09
9	0.81	0.84	0.48	0.28	0.40	0.83	-0.29	-0.14	1.00	-0.33	-0.34	0.82	-0.01	0.08	0.89	0.84	0.78	0.30	-0.24	-0.04	0.58	-0.40	0.31
10	-0.33	-0.34	-0.15	-0.59	-0.44	-0.28	0.39	0.33	-0.33	1.00	0.75	-0.38	0.37	0.31	-0.34	-0.35	-0.36	-0.15	0.31	0.31	-0.25	0.24	-0.14
11	-0.39	-0.37	-0.19	-0.46	-0.43	-0.33	0.31	0.43	-0.34	0.75	1.00	-0.36	0.26	0.37	-0.35	-0.39	-0.38	-0.15	0.39	0.41	-0.28	0.29	-0.12
12	0.81	0.82	0.48	0.43	0.38	0.70	-0.25	-0.18	0.82	-0.38	-0.36	1.00	-0.02	0.06	0.85	0.82	0.77	0.33	-0.24	-0.08	0.60	-0.40	0.32
13	0.10	0.10	0.39	-0.06	-0.05	0.10	0.66	0.43	-0.01	0.37	0.26	-0.02	1.00	0.76	-0.04	0.07	0.08	0.06	0.46	0.52	0.25	0.20	0.25
14	0.08	0.13	0.37	-0.09	-0.04	0.14	0.49	0.63	0.08	0.31	0.37	0.06	0.76	1.00	0.08	0.09	0.11	0.06	0.54	0.64	0.23	0.19	0.26
15	0.83	0.82	0.48	0.33	0.38	0.78	-0.27	-0.15	0.89	-0.34	-0.35	0.85	-0.04	0.08	1.00	0.85	0.77	0.30	-0.24	-0.05	0.59	-0.42	0.29
16	0.97	0.82	0.55	0.37	0.39	0.84	-0.22	-0.20	0.84	-0.35	-0.39	0.82	0.07	0.09	0.85	1.00	0.75	0.29	-0.24	-0.05	0.67	-0.48	0.27
17	0.73	0.90	0.60	0.33	0.42	0.78	-0.21	-0.17	0.78	-0.36	-0.38	0.77	0.08	0.11	0.77	0.75	1.00	0.41	-0.24	-0.03	0.73	-0.33	0.51
18	0.25	0.43	0.40	0.16	0.19	0.32	-0.03	-0.03	0.30	-0.15	-0.15	0.33	0.06	0.06	0.30	0.29	0.41	1.00	-0.05	0.06	0.40	-0.07	0.29
19	-0.24	-0.21	0.15	-0.03	-0.01	-0.19	0.64	0.76	-0.24	0.31	0.39	-0.24	0.46	0.54	-0.24	-0.24	-0.24	-0.05	1.00	0.85	0.01	0.35	0.07
20	-0.07	0.03	0.32	-0.14	-0.06	0.02	0.55	0.70	-0.04	0.31	0.41	-0.08	0.52	0.64	-0.05	-0.05	-0.03	0.06	0.85	1.00	0.19	0.26	0.20
21	0.63	0.76	0.76	0.32	0.36	0.65	0.01	-0.01	0.58	-0.25	-0.28	0.60	0.25	0.23	0.59	0.67	0.73	0.40	0.01	0.19	1.00	-0.20	0.51
22	-0.51	-0.37	-0.10	-0.15	-0.14	-0.40	0.34	0.34	-0.40	0.24	0.29	-0.40	0.20	0.19	-0.42	-0.48	-0.33	-0.07	0.35	0.26	-0.20	1.00	0.20
23	0.23	0.44	0.54	0.16	0.21	0.31	0.08	0.09	0.31	-0.14	-0.12	0.32	0.25	0.26	0.29	0.27	0.51	0.29	0.07	0.20	0.51	0.20	1.00

Table 4. PCA misclassification and percent variance explained for tornado cases.

Number of dimensions	Number of misclassifications	Percent variance	Percent of data
4	4	65.5	17.4
5	3	70.6	21.7
6	3	74.9	26.1
7	3	78.7	30.4
8	4	82.0	34.8
9	1	85.0	39.1
10	7	87.2	43.5

Table 5. PCA misclassifications and percent variance explained for non-tornado cases.

Number of dimensions	Number of misclassifications	Percent variance	Percent of data
4	8	74.9	17.4
5	6	78.5	21.7
6	8	81.9	26.1
7	8	84.9	30.4
8	9	87.1	34.8
9	13	89.2	39.1
10	10	91.0	43.5

Table 6. Coefficients of the highly loaded attributes on each dimension of tornado PC loadings.

Attribute	PC1	PC2	PC3	PC4	PC5	PC6	PC7	PC8	PC9
1		0.89							
2			0.70						
3	0.83								
4				-0.86					
5									-0.87
6			0.52						
7	0.86								
8	0.87								
9					0.78				
10	0.55			0.61					
11	0.62								
12					0.65				
13	0.80								
14	0.89								
15					0.82				
16		0.72			0.50				
17							0.90		
18						-0.99			
19	0.91								
20	0.87								
21			0.84						
22		-0.78							
23								0.83	
Variance explained (%)	27.4	11.5	5.2	8.1	11.6	4.3	5.0	4.1	4.7

Table 7. Coefficients of highly loaded attributes on each dimension of non-tornado PC loadings.

Attribute	PC1	PC2	PC3	PC4	PC5
1	0.91				
2	0.86				
3	0.52			-0.55	
4			-0.87		
5			-0.75		
6	0.88				
7		0.69			-0.50
8		0.91			
9	0.90				
10			0.73		
11			0.66		
12	0.84				
13					-0.79
14		0.66			
15	0.90				
16	0.92				
17	0.78				
18				-0.61	
19		0.90			
20		0.87			
21	0.63		0.84	-0.50	
22	-0.58				
23				-0.79	
Variance explained (%)	33.0	17.8	11.8	9.8	6.2

Table 8. Twelve most highly weighted attributes and their significance as determined by stepwise procedures in linear modeling.

Attribute	Value	t-value	P-value
1. strength rank	0.0624	13.2720	0.0000
2. age (min)	0.0030	8.8781	0.0000
3. core depth (m)	0.0000	7.4595	0.0000
4. relative depth (%)	0.0031	6.4183	0.0000
5. strength index (MSI) weighted by average density of integrated layer	0.0000	-5.4124	0.0000
6. low-level convergence (m/s)	0.0045	3.8674	0.0001
7. height of maximum gate-to-gate velocity difference (m)	0.0000	-3.8175	0.0001
8. maximum rotational velocity (m/s)	0.0069	3.6759	0.0002
9. base (m)	0.0000	-2.6967	0.0071
10. low-level diameter (m)	0.0000	2.6220	0.0088
11. depth (m)	0.0000	2.5289	0.0115
12. height of maximum rotational velocity (m/s)	0.0000	-2.0230	0.0432

Table 9. Nine most highly weighted attributes and their t-values determined by deviance in logistic modeling.

Attribute	Value	t-value
1. strength rank	0.4924404139	9.726077
2. age (min)	0.0280589433	7.593679
3. base (m)	-0.00037453005	-4.801720
4. core depth (m)	0.00024986112	4.657541
5. depth (m)	0.00012817021	3.696870
6. relative depth (%)	0.01355801282	3.375609
7. low-level diameter (m)	0.00007311782	2.778578
8. strength index (MSI) weighted by average density of integrated layer	-0.00020253292	-2.706315
9. low-level convergence (m/s)	0.02499769788	2.409429

Table 10. Regression results for linear and logistic modeling.

Regression method	# of correct classifications		Percent of total-correct		# of misclassifications		Percent of total-incorrect	
Linear	A	B	A	B	A	B	A	B
	1907	1890	84.4	83.7	352	369	15.6	16.3
Logistic	1914	1893	84.7	83.8	345	366	15.3	16.2

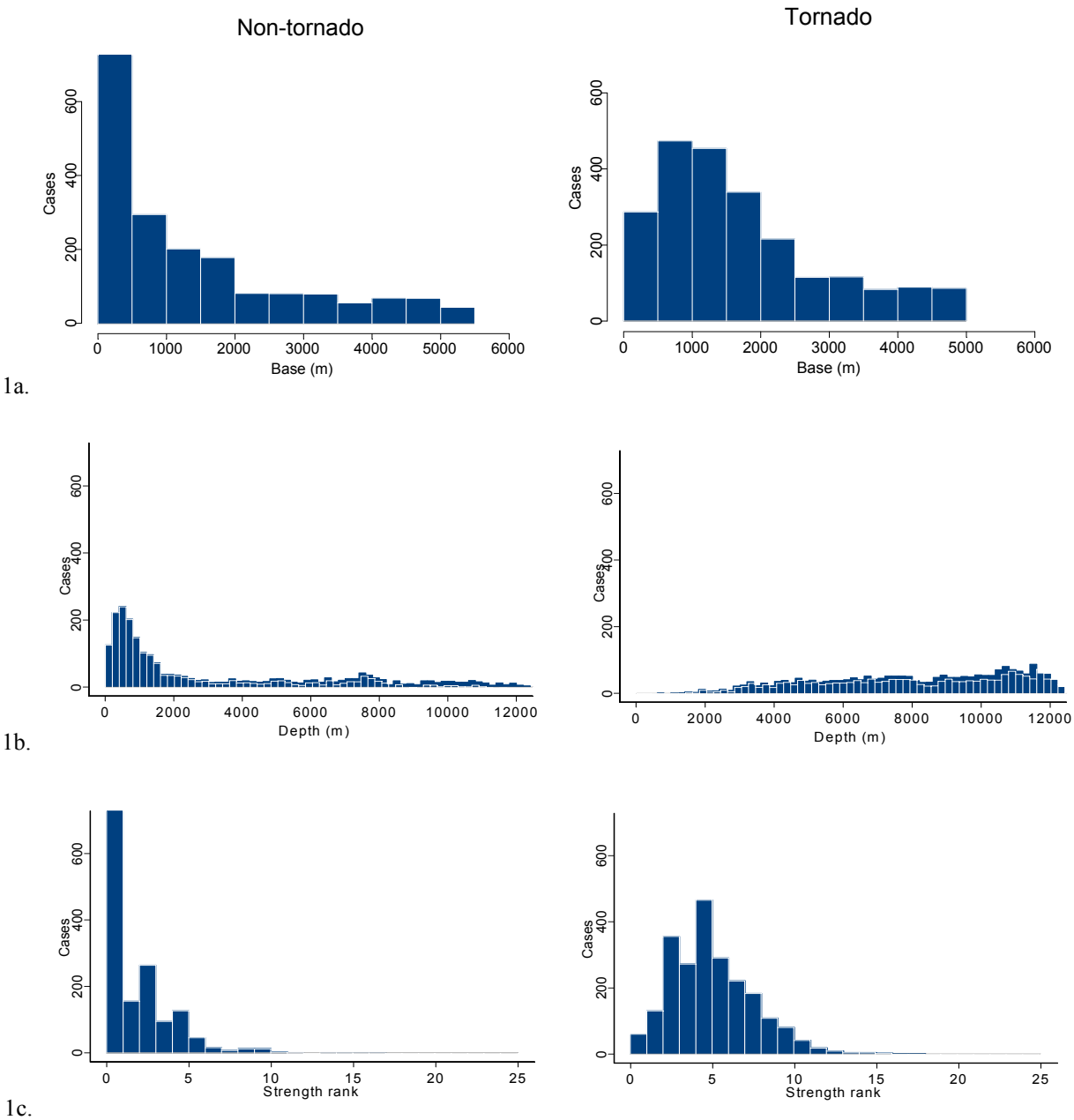

Figure 1. Histograms of tornado events (panels in left column) versus non-tornado events (panels in right column) for each of the 23 MDA attributes.

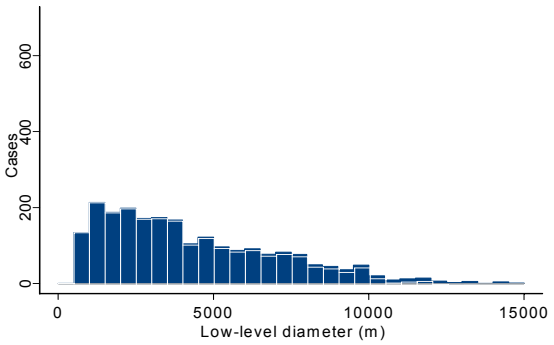

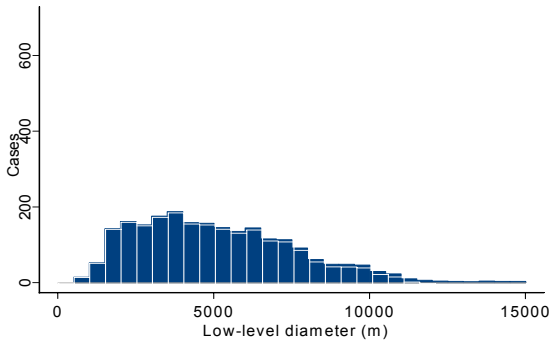

1d.

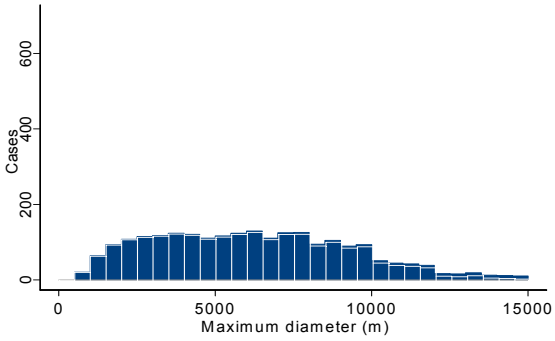

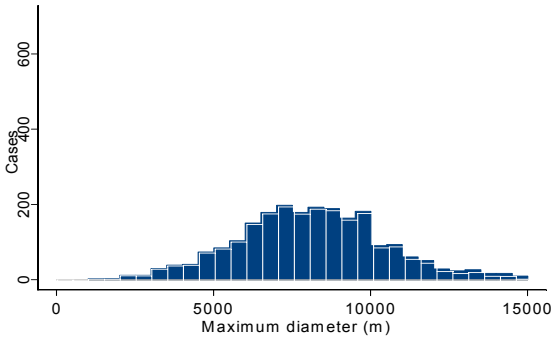

1e.

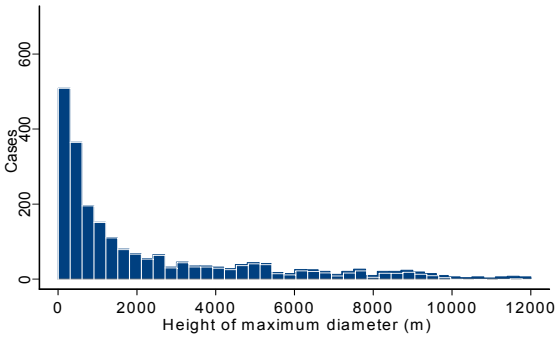

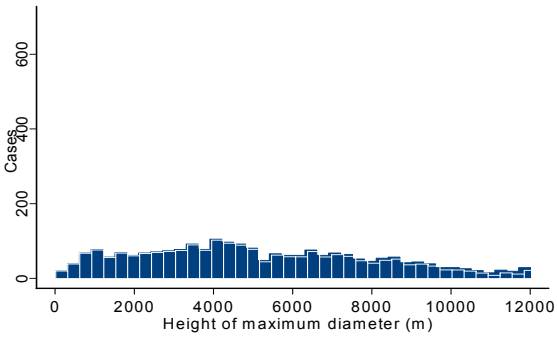

1f.

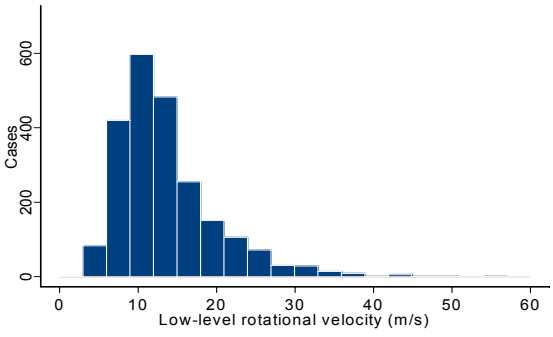

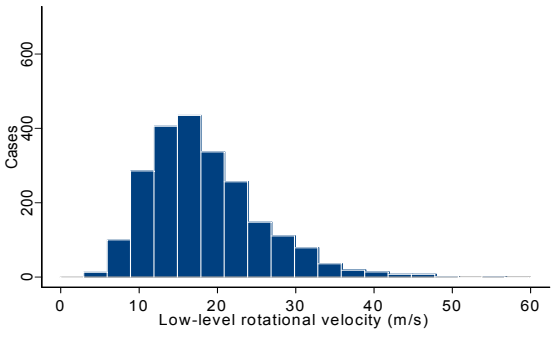

1g.

Figure 1. Continued.

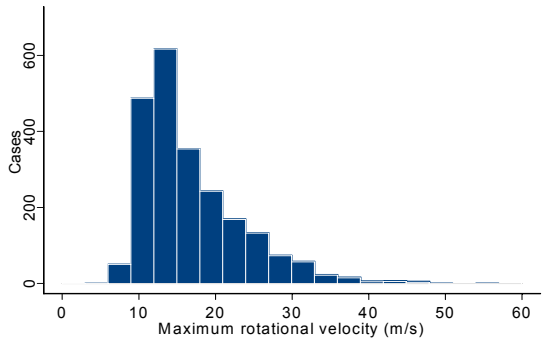

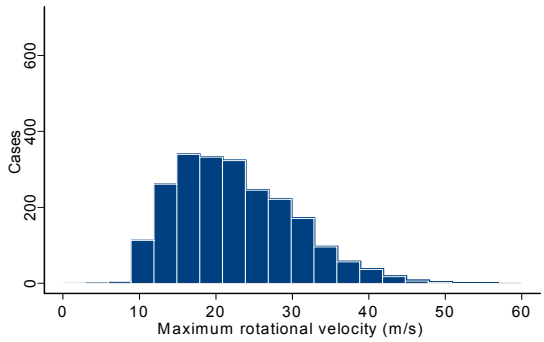

1h.

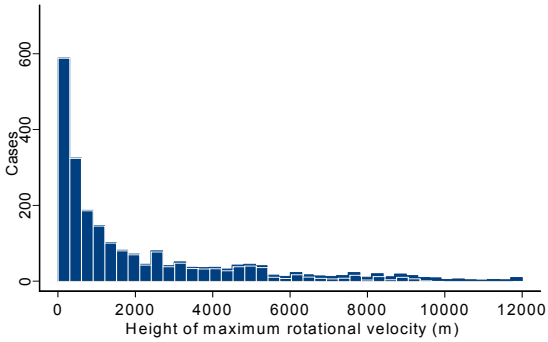

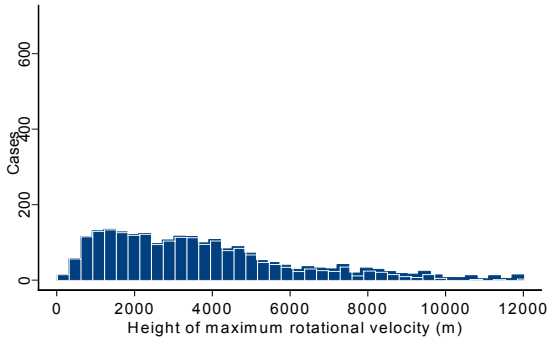

1i.

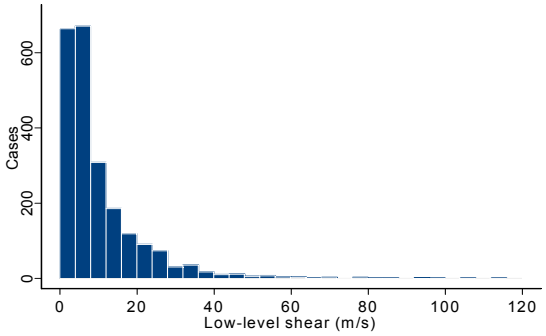

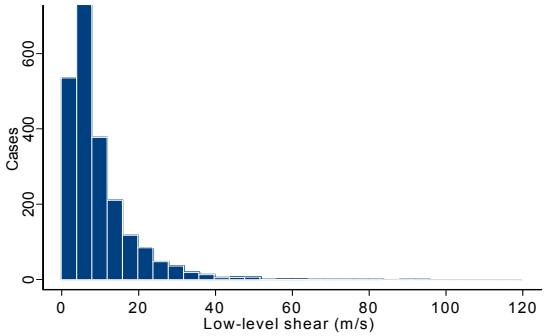

1j.

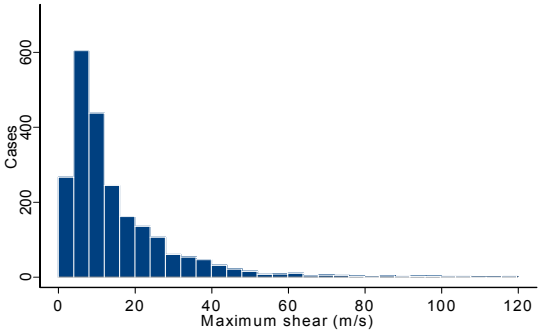

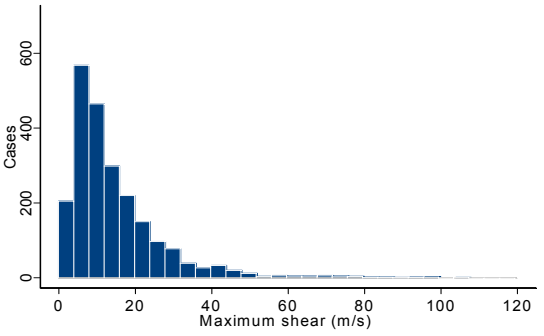

1k.

Figure 1. Continued.

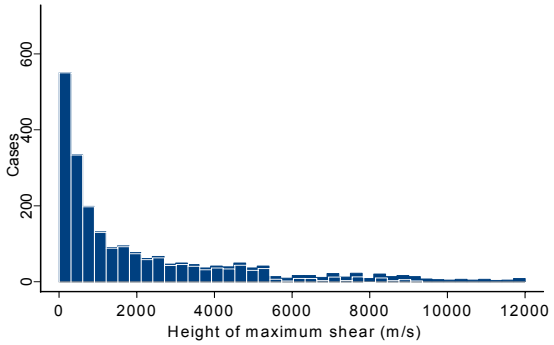

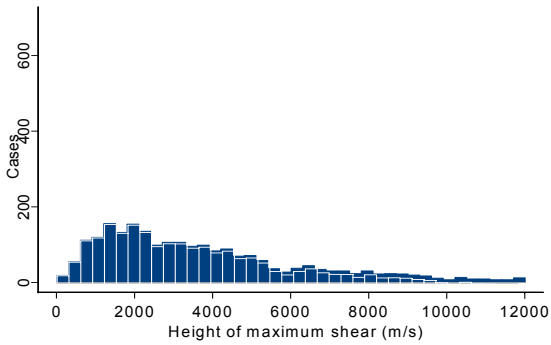

1l.

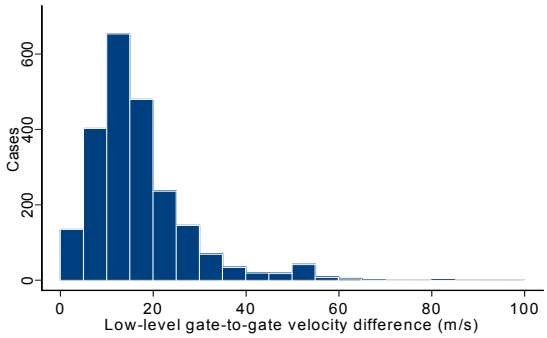

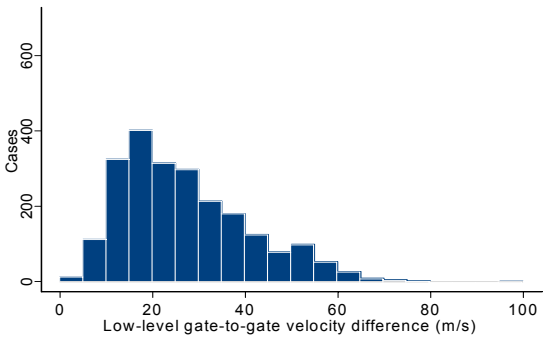

1m.

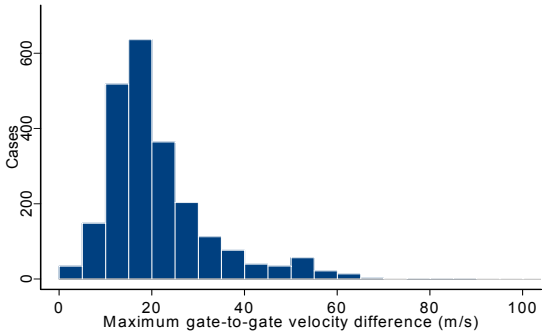

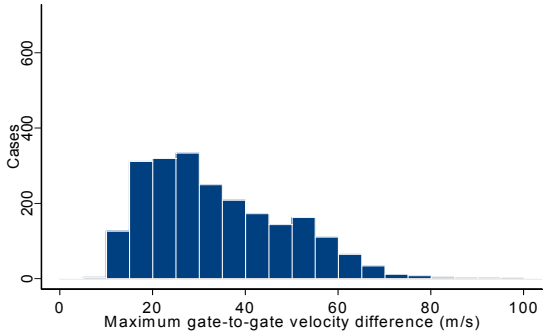

1n.

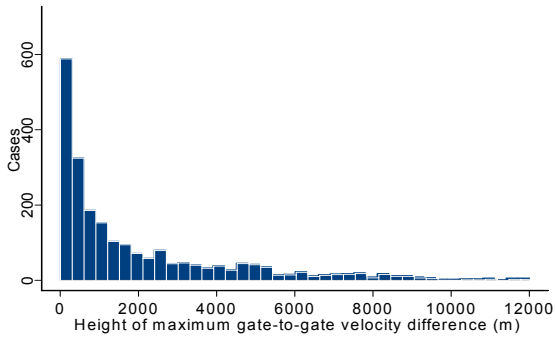

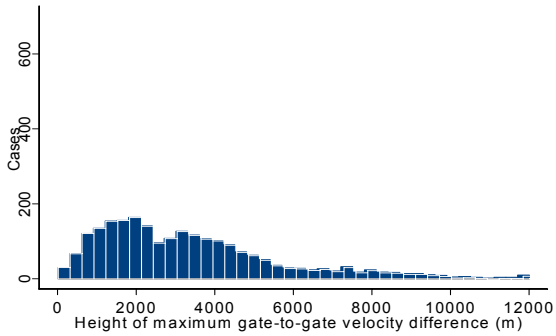

1o.

.

Figure 1. Continued.

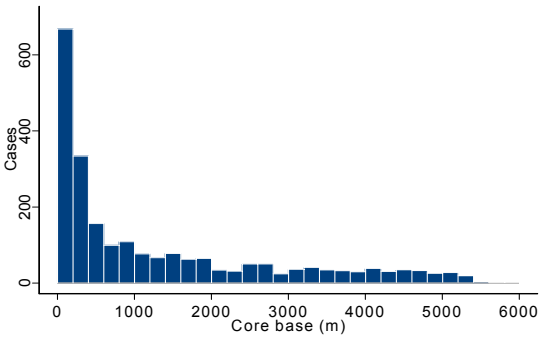

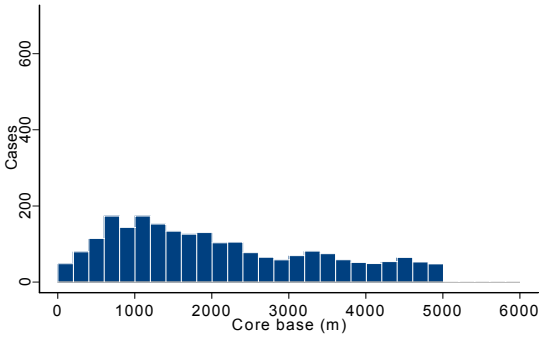

1p.

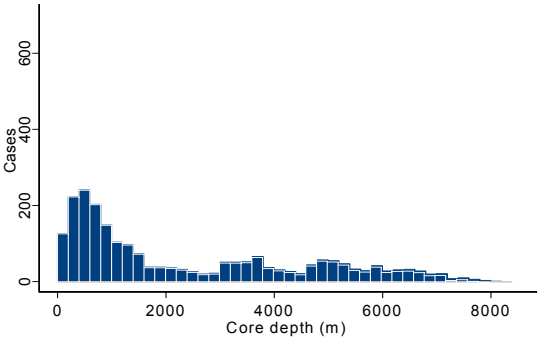

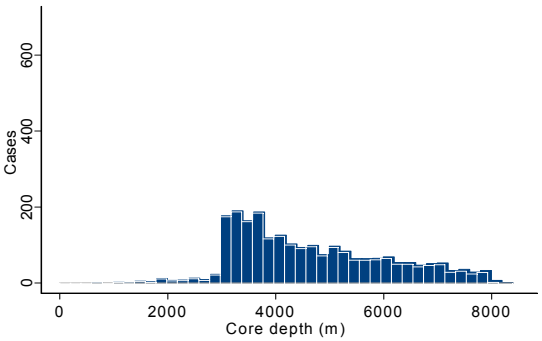

1q.

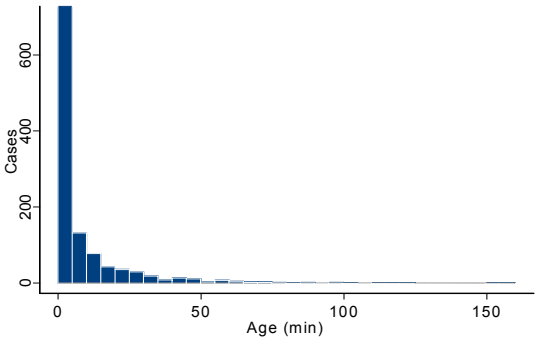

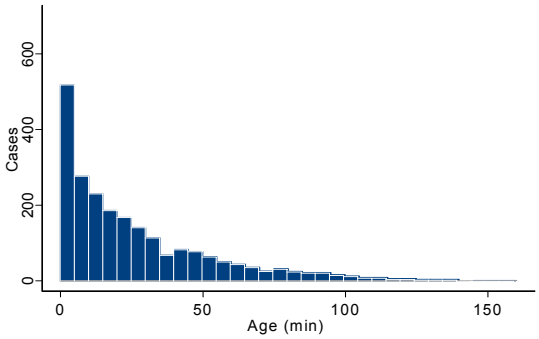

1r.

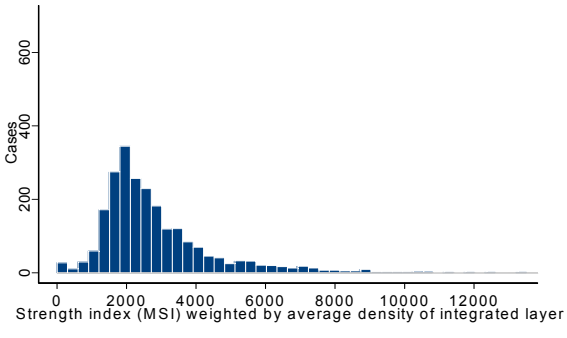

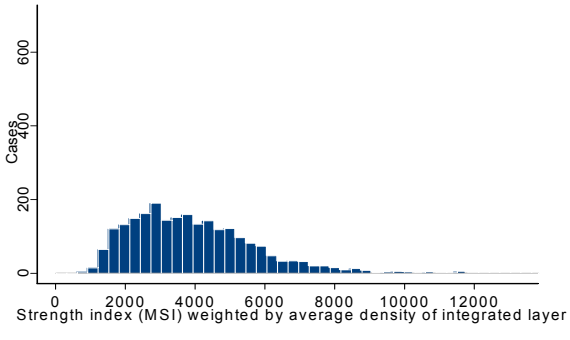

1s.

Figure 1. Continued

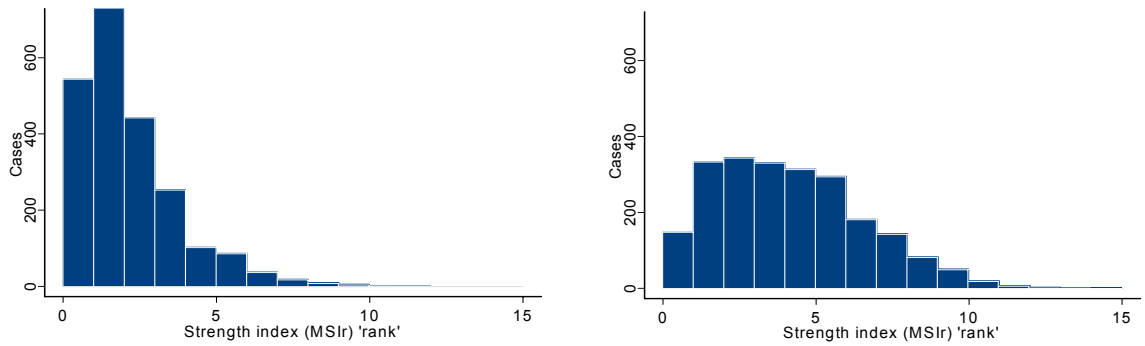

1t.

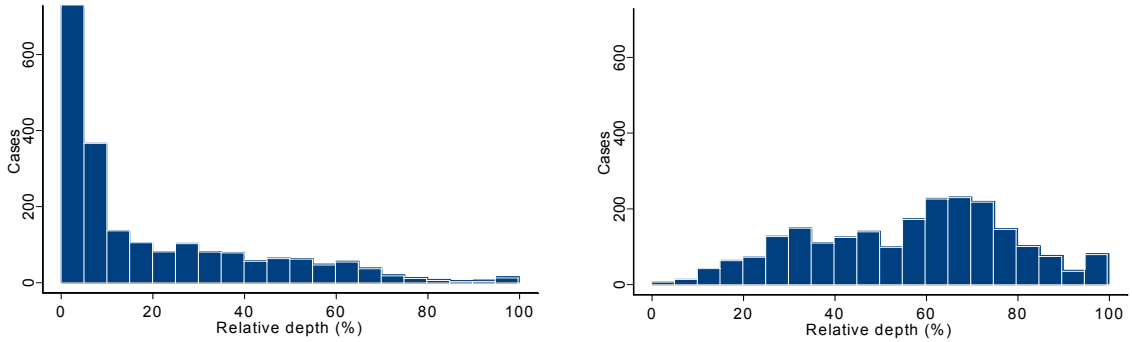

1u.

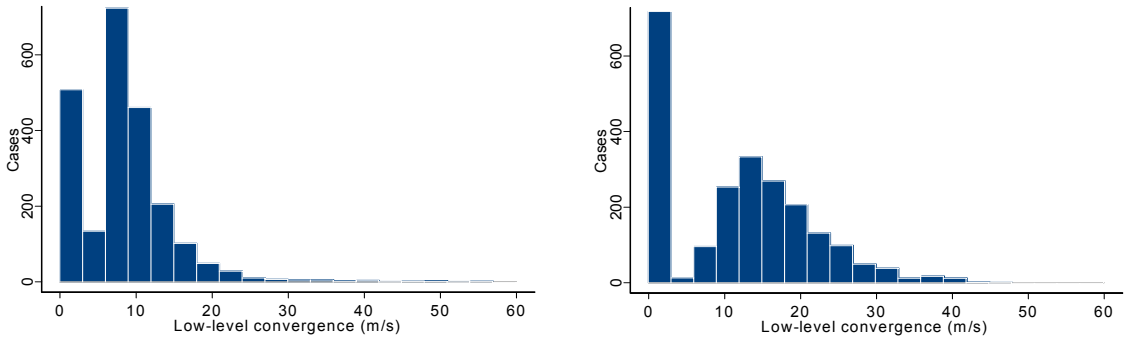

1v.

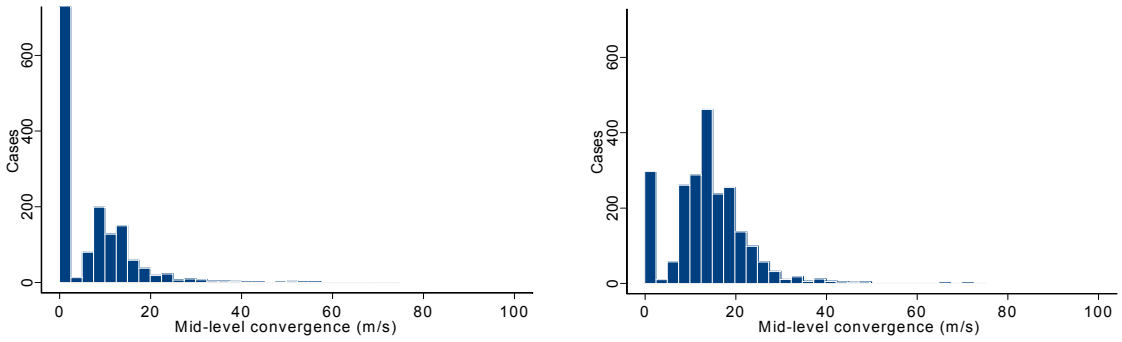

1w.

Figure 1. Continued.

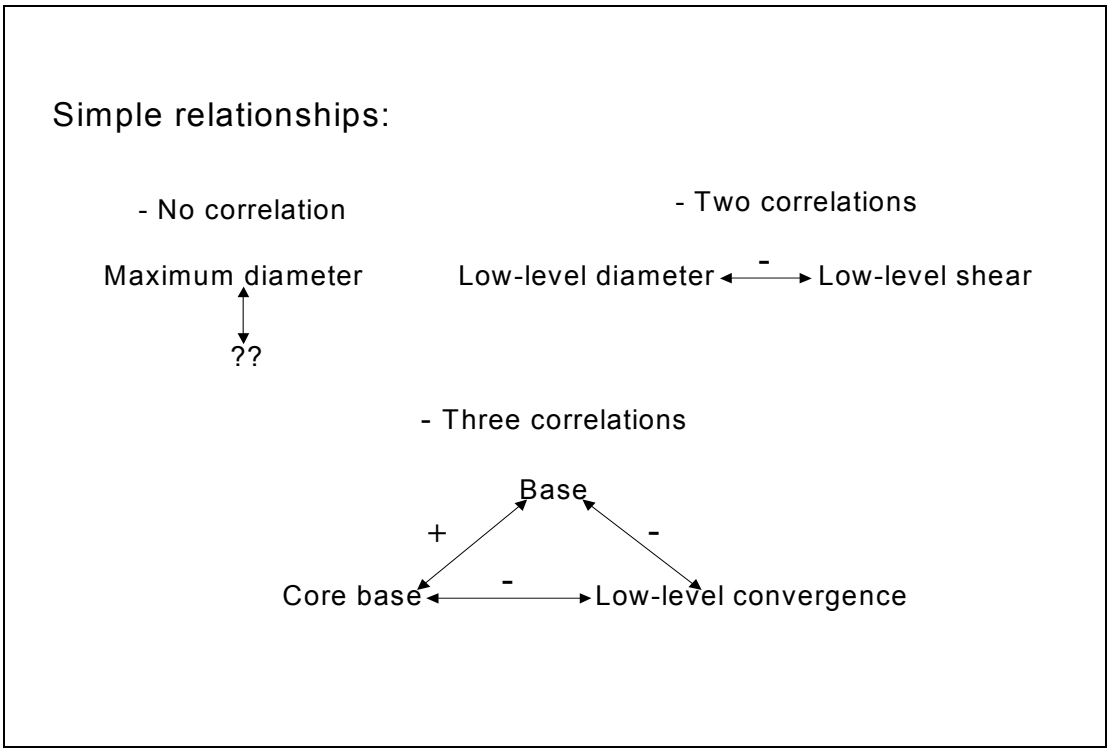

2a.

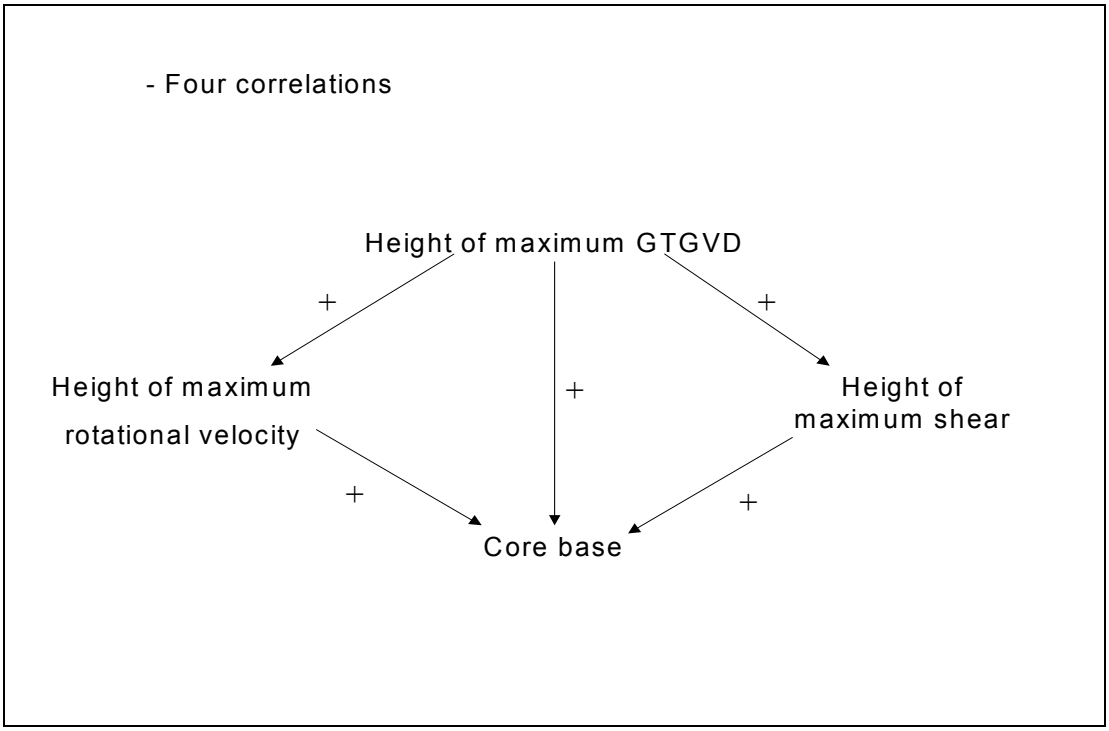

2b.

Figure 2. Different complexities of correlation relationships. Panel a has simple relationships, Panel b has moderate complexity, and Panel c illustrates a highly complex relationship.

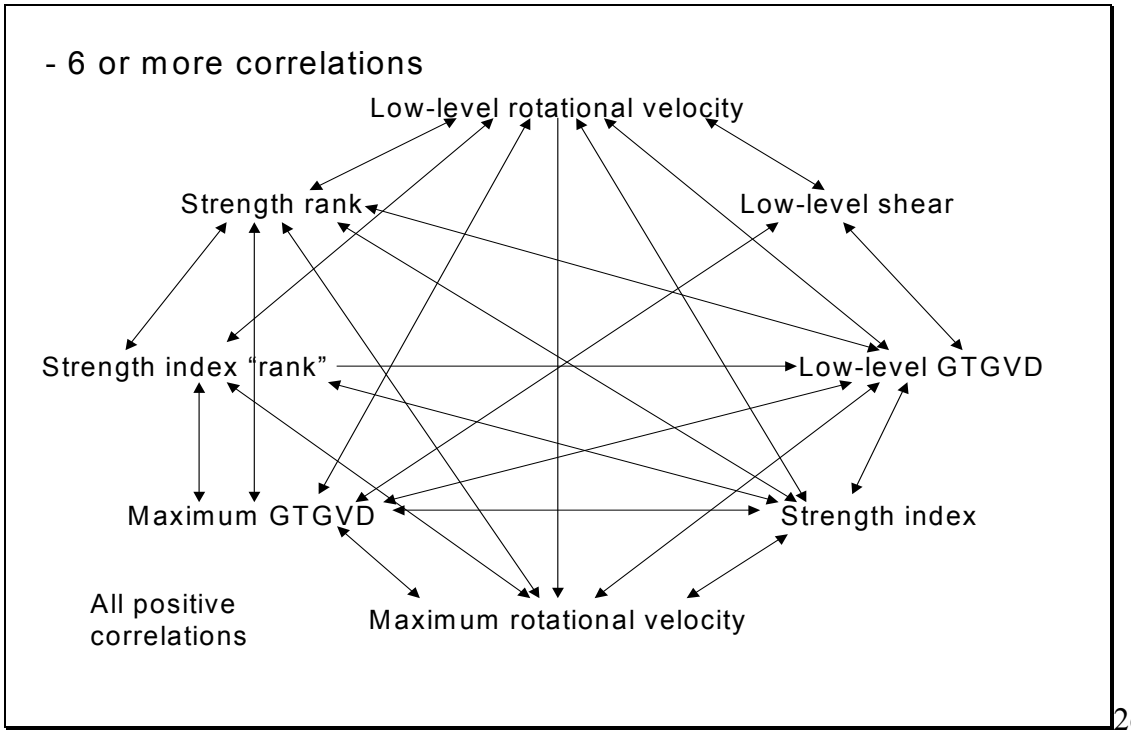

2c.

Figure 2. Continued.

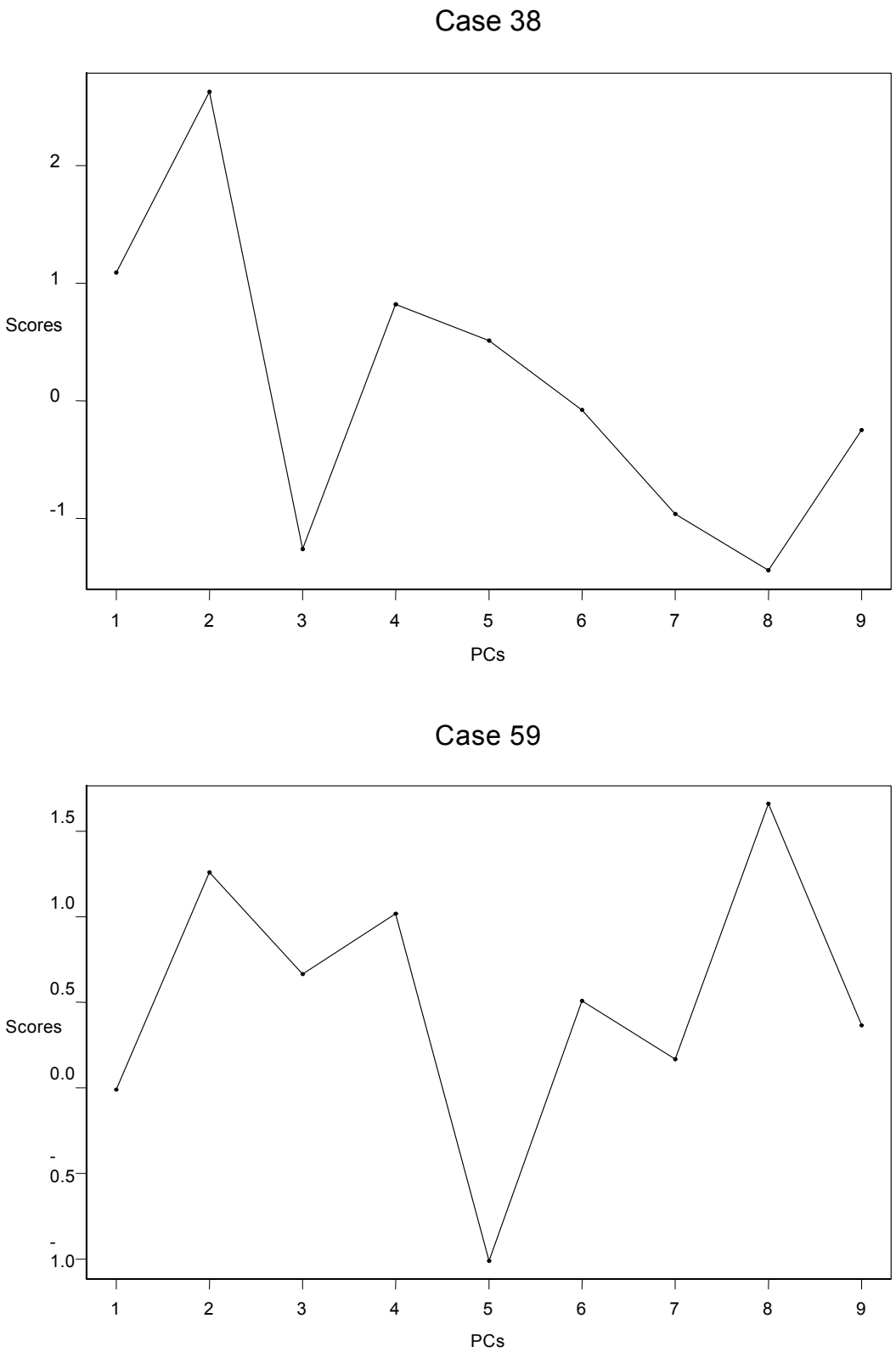

Figure 3. Individual tornado profiles showing the score on each PC.